

Low-temperature drying of waste activated sludge enhanced by agricultural biomass towards self-supporting incineration

Li, Ji; Hao, Xiaodi; Shen, Zhan; Wu, Yuanyuan; van Loosdrecht, Mark C.M.

DOI

[10.1016/j.scitotenv.2023.164200](https://doi.org/10.1016/j.scitotenv.2023.164200)

Publication date

2023

Document Version

Final published version

Published in

Science of the Total Environment

Citation (APA)

Li, J., Hao, X., Shen, Z., Wu, Y., & van Loosdrecht, M. C. M. (2023). Low-temperature drying of waste activated sludge enhanced by agricultural biomass towards self-supporting incineration. *Science of the Total Environment*, 888, Article 164200. <https://doi.org/10.1016/j.scitotenv.2023.164200>

Important note

To cite this publication, please use the final published version (if applicable).
Please check the document version above.

Copyright

Other than for strictly personal use, it is not permitted to download, forward or distribute the text or part of it, without the consent of the author(s) and/or copyright holder(s), unless the work is under an open content license such as Creative Commons.

Takedown policy

Please contact us and provide details if you believe this document breaches copyrights.
We will remove access to the work immediately and investigate your claim.

Green Open Access added to TU Delft Institutional Repository

'You share, we take care!' - Taverne project

<https://www.openaccess.nl/en/you-share-we-take-care>

Otherwise as indicated in the copyright section: the publisher is the copyright holder of this work and the author uses the Dutch legislation to make this work public.



Low-temperature drying of waste activated sludge enhanced by agricultural biomass towards self-supporting incineration

Ji Li ^a, Xiaodi Hao ^{a,*}, Zhan Shen ^a, Yuanyuan Wu ^{a,c}, Mark C.M. van Loosdrecht ^{a,b}

^a Sino-Dutch R&D Centre for Future Wastewater Treatment Technologies/Beijing Advanced Innovation Centre of Future Urban Design, Beijing University of Civil Engineering & Architecture, Beijing 100044, PR China

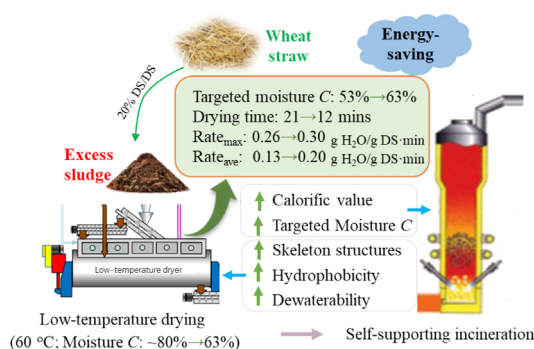
^b Dept. of Biotechnology, Delft University of Technology, van der Maasweg 9, 2629, HZ, Delft, the Netherlands

^c Beijing Capital Eco-Environment Protection Group Co., Ltd., Beijing 100044, PR China

HIGHLIGHTS

- Agricultural biomass was utilized to enhance the sludge drying efficiency.
- Adding crushed wheat straw of 20 % was efficient enough for the purpose.
- The drying time was shortened by almost a half at a 20 % adding ratio.
- Sludge dewaterability, hydrophobicity and mesh-like structures were improved.

GRAPHICAL ABSTRACT



ARTICLE INFO

Editor: Qilin Wang

Keywords:

Waste activated sludge (WAS)
Low-temperature drying
Agricultural biomass
Wheat straw
Targeted moisture content
Drying time

ABSTRACT

A high moisture content of waste activated sludge (WAS) associated with a low calorific value needs to be deeply dried towards self-supporting incineration. On the other hand, thermal energy with low temperature exchanged from treated effluent has great potential for drying sludge. Unfortunately, low-temperature drying of sludge seems to be low in efficiency and long in drying time. For this reason, some agricultural biomass was added into WAS to improve the drying efficiency. The drying performance and sludge properties were analyzed and evaluated with this study. Experimental results demonstrated that wheat straw was the best in enhancing the drying performance. With only 20 % (DS/DS) of crushed wheat straw added, the average drying rate achieved up to 0.20 g water/g DS-min, much higher than 0.13 g water/g DS-min of the raw WAS. The drying time to the targeted moisture content (63 %) (for self-supporting incineration) was shortened to only 12 min, much lower than 21 min of the raw WAS. The analysis revealed that wheat straw could reduce the specific resistance of filtration (SRF) and increase the sludge filterability (X). Also, the sludge rheology, particle size distribution and SEM images could conclude that agricultural biomass played a positive role in skeleton builders, forming a mesh-like structure in sludge flocs. These special channels could obviously improve the transfer capacities of heat and water inside the sludge matrix and thus greatly increase the drying performance of WAS.

1. Introduction

Waste activated sludge (WAS) from wastewater treatment plants (WWTPs) has greatly increased along with rapid industrialization and urbanization (Wang et al., 2018; Zhang et al., 2016). In this decade, handling WAS towards a circular economy has become an important theme. Some

* Corresponding author.

E-mail address: xdhao@hotmail.com (X. Hao).

traditional economical handling approaches like sludge landfill and agricultural applications have been gradually limited due to unavailable space and less-efficient fertilizer (Olga et al., 2022). Moreover, anaerobic digestion seems also ineffective in recovering organic energy and reducing sludge volume (Donatello and Cheeseman, 2013; Hao et al., 2019; Li et al., 2012; Zhang et al., 2016). Under the circumstance, direct incineration has been evaluated as an ultimate and environmental-friendly approach to sustainable WAS disposal due to maximal organic energy recovery, complete sludge reduction as well as highly efficient phosphate recovery from sludge incineration ashes (Donatello and Cheeseman, 2013; Hao et al., 2022; Hao et al., 2020; Wang et al., 2023).

However, the moisture content of WAS associated with the calorific value is a decisive factor for the self-supporting incineration process. A higher moisture content often results in more fuel consumption and thus more carbon emissions (Xiao et al., 2015). As a result, sludge dewatering and drying processes are certainly important before incineration, especially for self-supporting incineration. In this aspect, the Tanner diagram summarized by Komilis et al. (2014) is an efficient assessment tool to evaluate the calorific value of WAS for self-supporting incineration. Based on the Tanner diagram calculation, for example, the average organic content of WAS is around 53 % in China, and thus the moisture content needs to be decreased to at least 50 % which is the threshold value for self-supporting incineration (Hao et al., 2020). Therefore, dewatered sludge with a moisture content of 80 % needs to be deeply dewatered or dried to the targeted moisture content for self-supporting incineration. Although mechanical dewatering techniques are much easier, they always depend on advanced and complicated pre-treatment with chemical addition and heat supplies, which always cause high constructional and operational costs and also high energy consumption and carbon emissions. Moreover, these technologies would also worsen the incineration efficiency due to the negative effects on the sludge characteristics (Cao et al., 2021; Wu et al., 2020).

On the other hand, another effective and extensively practical strategy is the sludge drying technology by heat, but stable heat sources with low costs would be associated. Among them, waste heat from nearby power stations and/or heat boilers is often an ideal choice in practice. However, such cases are often not popular. Under the circumstance, in-situ low-grade thermal energy (50–60 °C) exchanged from the effluent of WWTPs gains more attention, which is a sustainable and clean energy for sludge drying (Hao et al., 2020; Hao et al., 2019). But a practical problem remains with the low-temperature drying process of sludge: it is low in efficiency or long in drying time. Thus, this study struggles with a strategy to resolve the problem.

Previous studies have concluded that chemicals are effective to improve the dewaterability of WAS (Chen et al., 2015; Niu et al., 2013; Qi et al., 2011). However, these common inorganic chemicals often lower the calorific value of conditioned sludge and thus deteriorate the efficiency of incineration. Other advanced conditioning techniques like Fenton oxidation, acid and alkali pretreatment are energy-intensive and not environmental-friendly in practice (Liu et al., 2013; Yang et al., 2013). On the other hand, Liu et al. (2017) found that adding sawdust chips could improve the dewatering performance and drying rate of WAS. Lin et al. (2001) also improved the sludge dewaterability by adding wood chips and wheat dregs. Wu et al. (2016) concluded that the settleability and dewaterability of sludge were improved with rice husk biochar. Indeed, these agricultural biomass could not only improve the efficiency of sludge dewatering and low-temperature drying, but could also increase the organic contents in WAS, which is of benefit for self-supporting incineration (Lin et al., 2001; Liu et al., 2017; Wu et al., 2016). Although these key parameters such as CST, SRF and viscosity of excess sludge have been analyzed and some positive enhancement has already been concluded in these studies, the performance of the low-temperature drying and the feasibility of self-supporting incineration of excess sludge by conditioning with different biomass were still vague. Thus, this study evaluated the low-temperature drying as well as the incineration process enhanced by different agricultural biomass towards energy saving and recovery from excess sludge.

With this study, three different agricultural biomass, cypress sawdust, maize cob and wheat straw, were applied in WAS drying process as organic conditioners. Different types and added ratios of agricultural biomass affecting the low-temperature drying performance of WAS were investigated and analyzed. Moreover, sludge dewaterability, rheological and morphological properties, hydrophobicity and particle size distribution were also evaluated to clarify the synergistic enhancement and the associated mechanisms.

2. Materials and methods

2.1. WAS and agricultural biomass

WAS was collected from a municipal WWTP in Beijing, China and stored in a fridge (4 °C) for use. The characteristics of the concentrated WAS are listed in Table 1. Three different agricultural biomass, cypress sawdust, maize cob and wheat straw were chosen as the organic conditioners to improve the efficiency of sludge dewatering and drying processes. The previous results showed that the biomass with the normal size distribution achieved the greatest effect on the drying performance than those with different specific sizes. Thus, crushed biomass with the normal size distribution (0.1–2 mm) was applied directly in the study.

2.2. Experimental set-up

The detailed procedures of the experiment are depicted in Fig. 1. Different agricultural biomass and designed added ratios (0–100 %, dry solid/dry solid) were first poured into raw WAS and completely mixed at 1000 rpm for 10 min. Then, some mixed samples were measured for some parameters including capillary suction time (CST), specific resistance of filtration (SRF), rheological properties and others. Next, the rest of the mixed samples were mechanically dewatered by press filtration to obtain sludge cakes with the moisture content of around 80 %. Finally, the cakes were shaped into 2.0-mm diameter strips by a spiral extrusion-molding machine, which automatically recorded the drying performance by Halogen rapid moisture detector (0.005 g, YLS-16, China). The drying temperature is set at a constant temperature of 60 °C, which is the economical available condition that can be maintained in practice by the thermal energy extracted from effluent via wastewater heat source pumps (WHSP).

2.3. Analytical assessment methods

2.3.1. Dewaterability and filterability

Capillary suction time (CST) and specific resistance of filtration (SRF) are measured to evaluate the dewaterability of sludge. CST represents the specific time of the filtrate traveling a fixed distance on a special filter paper. A high CST value means poor filterability and dewaterability. Due to the influences of different added biomass on the viscosity, the sludge filterability constant (X, described by Vesilind; Cetin and Erdinciler) (Cetin

Table 1

Characteristics of the concentrated waste activated sludge (WAS) used in this study.

Parameters	Value	Parameters	Value
MLSS (g/L) ^A	30.2 ± 0.2	CST (s) ^C	245.4 ± 43.6
MLVSS (g/L) ^B	16.0 ± 0.1	SRF (m/kg) ^D	6.38E+12
MLVSS/MLSS	0.53	MV (μm) ^E	46.3 ± 0.2
Moisture content	96.5 % ± 0.6 %	CS (m ² /cm ³) ^F	0.19 ± 0.05
pH	7.1 ± 0.1	D[50] (μm) ^G	37.2 ± 0.2
Viscosity (mPa·s)	20.8 ± 1.3	D[95] (μm) ^G	14.3 ± 1.6

^A MLSS, Mixed liquor suspended solids; ^B MLVSS, Mixed liquor volatile suspended solids; ^C CST, Capillary suction time; ^D SRF, Specific resistance of filtration; ^E MV, Mean diameter of the volume distribution, μm; ^F CS, Calculated specific surface area, m²/cm³; ^G D[50] and D[90], Particle parameter representing cumulative 50 % and 90 % distribution of a cumulative curve, respectively, μm.

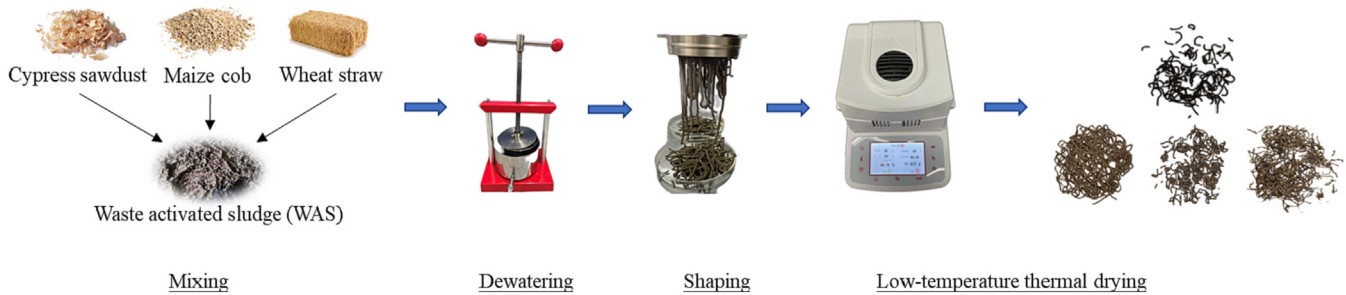


Fig. 1. Detailed procedures of sludge samples pretreatment and drying process.

and Erdinciler, 2004; Vesilind, 1988), should be calculated to optimize the CST analysis:

$$X = \phi \mu \frac{SS}{CST} \quad (1)$$

where, X —filterability constant, $\text{kg}^2/\text{m}^4 \cdot \text{s}^2$;

ϕ —a dimensionless constant characteristic of the CST apparatus (0.118 in the study);

μ —water viscosity, $\text{kg}/\text{s} \cdot \text{m}$; ($\mu_{\text{water}} = 0.890 \times 10^{-3} \text{ kg}/\text{s} \cdot \text{m}$ at 25°C);

SS —sludge solids concentration, kg/m^3 ;

CST —capillary suction time, s.

SRF represents the specific resistance per unit volume of filtrate through per filter area. In this study, 100 mL of sludge sample was poured into a Buchner funnel filled with $0.45\text{-}\mu\text{m}$ filter paper. Then, the constant pressure (0.06 MPa) was maintained by a vacuum filtration device (SHZ-D-III). The filtrate volume was continuously recorded along with the filtration time. The endpoint was that some cracks appeared on the surface of the filter cake. SRF can be finally obtained by the calculations according to Eqs. (2) and (3) (Agerbaek and Keiding, 1993; Chen et al., 2015; Zhang et al., 2014).

$$\frac{t}{V} = b \cdot V + a \quad (2)$$

$$SRF = \frac{2P \cdot A^2 \cdot b}{u \cdot \omega} \quad (3)$$

where, SRF —specific resistance to filtration per unit volume of filtrate through per filter area, cm/kg ;

V —filtrate volume, cm^3 ;

t —filtration time, s;

a, b —interception and slope of a curve, respectively, obtained by plotting the ratio of the filtration time to the filtrate volume (t/V) versus the filtrate volume (V);

P —filtration pressure, Pa; constant value at 0.06 MPa in this study;

A —filter area, cm^2 , 63.6 cm^2 in this study;

u —filtrate viscosity, Pa·s;

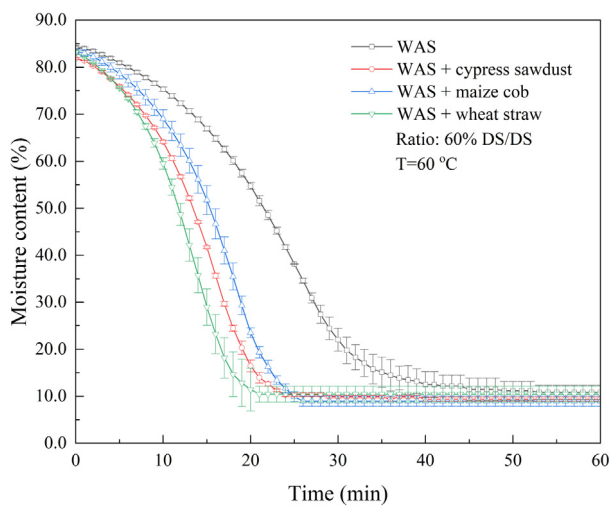
ω —dry solid weight per unit volume sludge, g/cm^3 .

2.3.2. Rheology properties

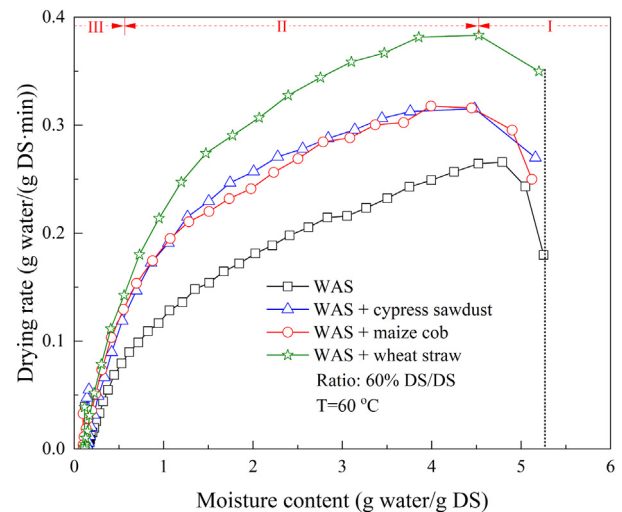
The rheology properties of sludge were performed by a rheometer (Haake Viscotester 550, Germany) in conjunction with the software recording the rheology process and data. A constant temperature was maintained at 25°C by a Peltier control. Rheological testing modes were referred to as follows: (i) maintaining a constant shear rate at 1000 s^{-1} lasting for 180 s; (ii) increasing the shear rate in a logarithm manner from 1 to 1000 s^{-1} . Rheograms of shear stress and viscosity as a function of shear rate were depicted and analyzed for rheology properties.

2.3.3. Characteristics analysis

The chemical functional groups of sludge were detected by a Fourier transform infrared spectrometer (FT-IR, Nicolet iS5, Thermo-Fisher Scientific). The spectra were measured at the wavenumber from 4000 to 400 cm^{-1} with KBr pellets (98 mg KBr + 2 mg sample). Morphological properties were also characterized using a scanning electron microscope (SEM) (G300, Zeiss German). Moreover, the particle size distributions and specific surface area of samples were analyzed by a laser particle size analyzer (Microtrac S3500, American Mickey Co., Ltd./USA). Other



(a) Moisture content



(b) Drying rate

Fig. 2. Drying performance of waste activated sludge (WAS) conditioned with agricultural biomass: (a) moisture content; b) drying rate.

Table 2

Evaluation of the drying performance of waste activated sludge (WAS) conditioned with agricultural biomass.

Samples	Peak point (min)	Drying rate (g water/(g DS·min))		Self-supporting incineration		Total time (min)
		Max.	Ave.	Targeted moisture content	Time (min)	
Raw WAS	3.0	0.26	0.13	53.1 %	21.0	39.0
+ Cypress sawdust	2.0	0.32	0.21	73.2 %	6.0	23.0
+ Maize cob	2.0	0.32	0.20	72.9 %	8.5	25.0
+ Wheat straw	2.0	0.34	0.23	73.2 %	6.0	20.0

parameters including MLSS, MLVSS, and pH were detected according to the standard methods (APHA, 2012).

2.3.4. Drying performance evaluation

The moisture content can be calculated by Eq. (4) (Tahmasebi et al., 2011). The average drying rate can be also calculated with the weight difference of sludge samples between the initial (W_{s,t_1}) and endpoint (W_{s,t_2}), based on Eq. (5). The value of ($t_2 - t_1$) was the total time of the drying period.

$$M_{DS} = \frac{W_S - W_{DS}}{W_{DS}} \quad (4)$$

$$r = \frac{W_{s,t_1} - W_{s,t_2}}{W_{DS}} / (t_2 - t_1) \quad (5)$$

where, r —drying rate, the weight of evaporated water per unit dry sample per minute, g water/(g DS·min);

M_{DS} —moisture content, g water/g DS;

W_{DS} —the dry solid weight of the sample, g DS;

W_S —the weight of sludge including water and dry solid, g;

W_{s,t_1} , W_{s,t_2} —weight of sludge at the time points of t_1 and t_2 , respectively, g;

t_1 , t_2 —time, min.

The principles of self-supporting incineration referred to the updated Tanner diagram as described in Komilis et al. (2014). Different types and ratios of agricultural biomass increased the calorific value of WAS. Based on the following Eq. (6), therefore, Q_{SH}' is obtained to calculate the calorific value of conditioned WAS. In Eq. (6), Q_{SH} and Q_A are the calorific value of raw WAS and different agricultural biomass, respectively, which are

obtained from the previous studies as listed in Table S1. r represents the ratio of agricultural biomass, %DS/DS.

$$Q_{SH}' = \frac{Q_{SH} + Q_A \times r}{1 + r} \quad (6)$$

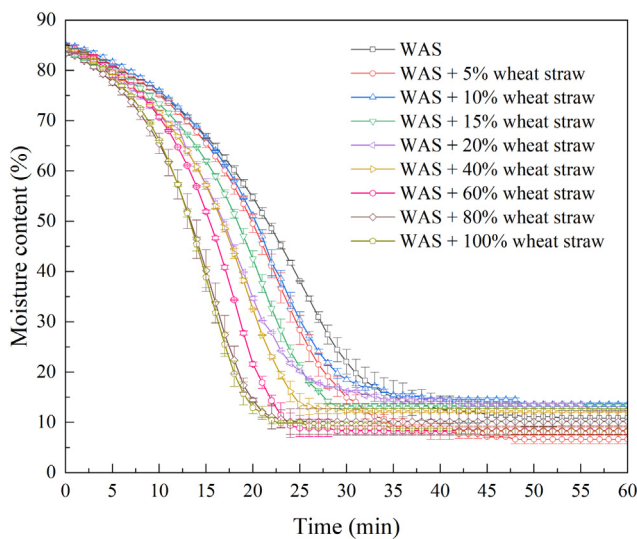
3. Results and discussion

3.1. Drying performance

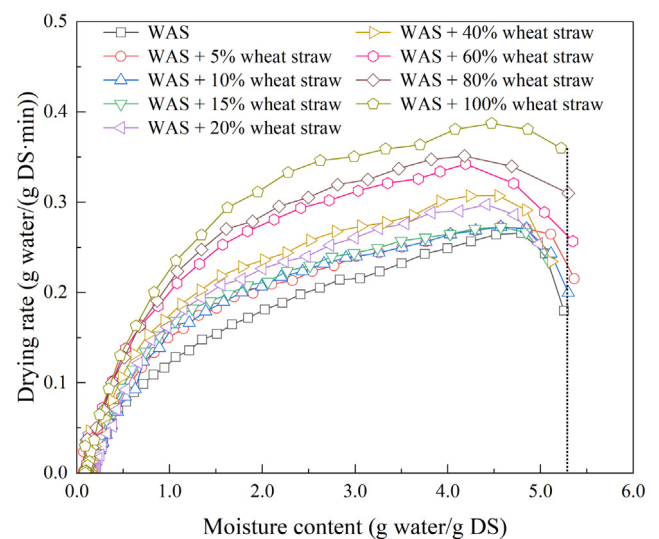
3.1.1. Effect of different agricultural biomass

The drying performance of WAS conditioned with different agricultural biomass are shown in Fig. 2a. The drying rate was calculated based on Eqs. (4) and (5) as described in Section 2.3.4 and the results are depicted in Fig. 2b. The whole drying process can be divided into three different phases: I) the increasing temperature phase, the heat was gradually transferred via the sludge strips, causing the increase of sludge temperature, and the drying rates climbed up to their peak points at the end of this phase; II) constant temperature drying phase, the drying rates slightly declined due to a large amount of water continuously released from sludge; III) slowly drying phase, the drying rate declined to ≤ 2.0 g water/(g DS·min), approaching to the drying endpoint.

The drying rates at $T = 60^\circ\text{C}$ of the conditioned sludge samples (DS/DS = 60 %) are calculated and listed in Table 2. The maximal drying rates (0.32, 0.32 and 0.34 g water/g DS·min) of the three conditioned sludge samples are higher than that of the raw sludge sample (0.26 g water/g DS·min). Moreover, the time reaching up to this maximal drying rate is 3.0 min for the raw sludge sample, compared to 2.0 min for the three conditioned sludge samples. As for the average drying rates, the



(a) Moisture content



(b) Drying rate

Fig. 3. Drying performance of waste activated sludge (WAS) conditioned with different ratios of wheat straw: a) moisture content; b) drying rate.

Table 3

Evaluation of the drying performance of waste activated sludge (WAS) conditioned with different ratios of wheat straw.

Samples	Peak point (min)	Drying rate (g water/(g DS·min))		Self-supporting incineration		Total time (min)
		Max.	Ave.	Targeted moisture content	Time (min)	
Raw WAS	3.0	0.26	0.13	53.1 %	21.0	39.0
+ 5 %	3.0	0.27	0.15	55.9 %	18.5	35.0
+ 10 %	3.0	0.28	0.17	58.3 %	18.0	32.0
+ 15 %	3.0	0.29	0.18	60.5 %	14.5	28.0
+ 20 %	3.0	0.30	0.20	62.5 %	12.0	26.0
+ 40 %	3.0	0.31	0.23	69.0 %	11.0	25.0
+ 60 %	3.0	0.34	0.23	73.2 %	6.0	20.0
+ 80 %	3.0	0.35	0.25	77.0 %	5.5	21.0
+ 100 %	3.0	0.39	0.26	79.0 %	4.5	20.0

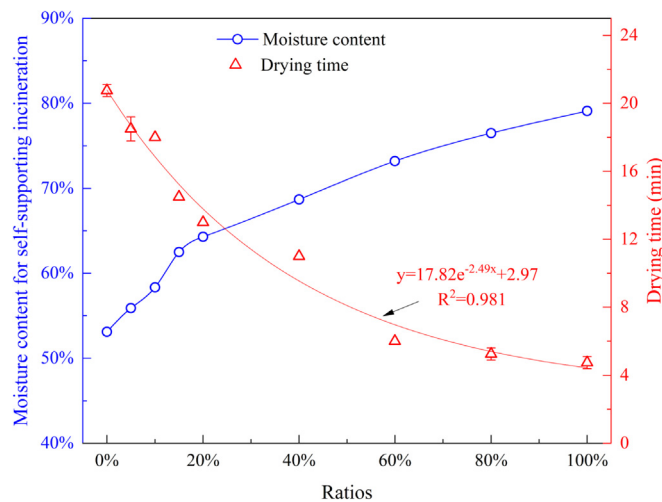


Fig. 4. Nonlinear fitting analysis of the relationship among the added ratios of wheat straw, the targeted moisture content and the drying time reaching to moisture content of self-supporting incineration.

three conditioned sludge samples are almost two higher (0.21, 0.20 and 0.23 water/g DS·min) than that of the raw sludge sample (0.13 water/g DS·min). Moreover, the drying time (down to the lowest moisture content, ~10 %) of the conditioned sludge samples is shorter (20–25 min) than that of the raw sludge samples (39 min). Thus, it can be concluded that the sludge drying performance can be significantly enhanced by agricultural biomass. Among three agricultural biomass, wheat straw was testified to be the optimal one for enhancing the drying efficiency, followed by cypress sawdust and maize cob.

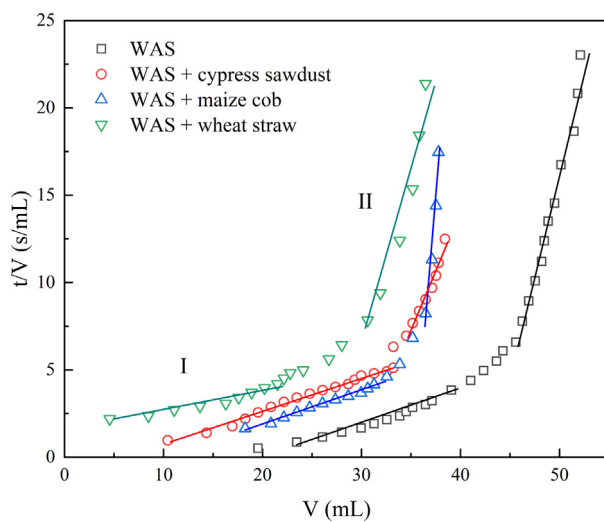
Towards self-supporting incineration, the targeted moisture content of the sludge samples were also evaluated according to the Tanner diagram, as described in [Section 2.3.4](#) (Hao et al., 2020; Komilis et al., 2014). As listed in [Table 2](#), the targeted moisture content of the raw WAS is 53.1 %, and the drying time was longer than 21 min. On the other hand, the calorific value of the conditioned sludge could be improved due to adding agricultural biomass with relatively higher calorific values. Hence, the targeted moisture content for the conditioned sludge samples increased to around 73 %, and thus the drying time was sharply shortened to about 6, 8.5 and 6 min, respectively.

In a word, it can be concluded that agricultural biomass can put a positive effect on the sludge dewatering and drying processes. On the other words, agricultural biomass can also significantly increase the calorific value of sludge and then shorten the drying time for self-supporting incineration.

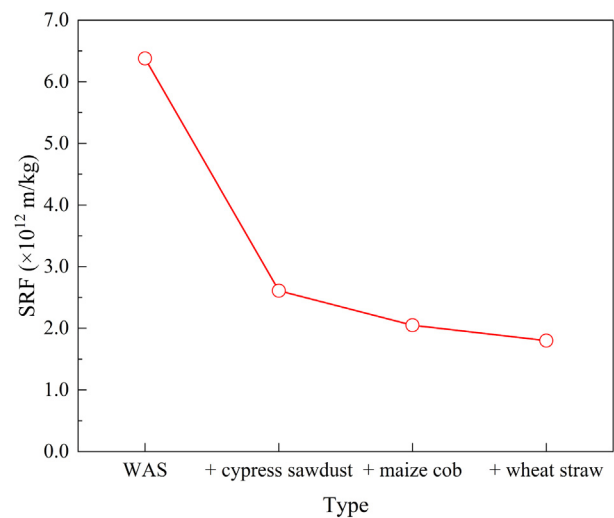
3.1.2. Effect of different added ratios

The effect of different added wheat straw ratios on the sludge drying performance was continuously investigated, which is shown in [Fig. 3](#) and [Table 3](#). The more wheat straw was added, the higher the sludge drying performance and efficiency achieved. At the added ratio of 100 %, the maximal and average drying rates reached up to 0.39 and 0.26 g water/(g DS·min), respectively, which were higher than that of the raw sludge sample (0.26 and 0.13 g water/g DS·min).

To quantitatively evaluate the effect of the added wheat straw ratios on self-supporting incineration, the nonlinear fitting analysis by SPSS software was applied to simulate the relationship among the added ratios, the targeted moisture content and the drying time reaching the moisture content of self-supporting incineration. As shown in [Fig. 4](#), the targeted moisture content for self-supporting incineration could increase along with the increase of the biomass dosage. However, the drying time fitted very well



(a)



(b)

Fig. 5. Filtration processes of the conditioned sludge samples: a) ratio of filtration time to filtrate volume (t/V) versus filtrate volume (V); b) specific resistance of filtration (SRF).

Table 4

Evaluation of the filtration processes of the conditioned sludge samples.

Samples	u (mPa·s)	V (cm ³)	m (g)	ω (g/cm ³)	b (s/cm ⁶)	SRF (m/kg)
WAS	20.8 ± 1.3	58.6	4.9	0.08	0.23	6.38E+12
WAS + cypress sawdust	21.7 ± 0.3	40.4	6.6	0.16	0.19	2.61E+12
WAS + maize cob	25.3 ± 0.6	37.8	7.7	0.20	0.22	2.05E+12
WAS + wheat straw	23.2 ± 0.2	37.1	6.8	0.18	0.16	1.80E+12

with the exponential relationship ($R^2 = 0.98$), which demonstrates that the drying performance became slowly enhanced with over 60 % of wheat straw. For example, 80 % of the added wheat straw ratio could only shorten 0.5 min (total 5.5 min) of the drying time, compared to 60 % of wheat straw (6.0 min).

Moreover, a higher moisture content always hinders the sludge fluidizing and reshaping, which is not supportive and economical for incinerators. Also, high dosages of biomass refer to high costs because of the sludge transportation and storage. Thus, based on these results and analysis, the raw WAS conditioned with the dosage of 20 % associated with the targeted moisture content at around 65 %, is the preferable condition for the incineration process. For this reason, 20 % of the added wheat straw ratio was proposed as the optimal ratio for enhancing the sludge drying performance, which were associated with the maximal and average drying rates of 0.30 and 0.20 g water/g DS·min respectively and also with a shortened drying time (12 min) to the targeted moisture content for self-supporting incineration, much shorter than the raw sludge (21.0 min).

3.2. Dewaterability enhanced

The processes of sludge filtration with different agricultural biomass added are depicted in Fig. 5a: I) rapid suction filtration stage, water molecules were quickly separated and released from sludge flocs; II) compacted stage, sludge was compacted to form sludge cakes under the high constant pressure. As described in Eqs. (2) and (3), the curve slope (b) of t/V (the ratio of filtration time to filtrate volume) versus V (filtrate volume) in the filtration process was plotted to calculate the value of SRF (Agerbaek and Keiding, 1993; Chen et al., 2015), which are shown in Fig. 5b and Table 4. SRF of the raw sludge sample was at the highest level, up to 6.38×10^{12} m/kg, compared to 1.80, 2.61 and 2.05×10^{12} m/kg for the conditioned sludge samples with wheat straw, cypress sawdust and

maize cob, respectively, about 59.1 %–72.8 % decreased. Clearly, agricultural biomass could improve the sludge dewaterability as a lower value of SRF is associated with better dewaterability (Zhang et al., 2014).

CST is also a critical parameter to evaluate the sludge dewaterability. As described in Section 2.3.1, the filterability constant (X , normalized CST) is calculated and shown in Fig. 6 (Cetin and Erdinciler, 2004; Vesilind, 1988). X value of the raw sludge was only $1.28 \times 10^{-5} \text{ kg}^2/\text{m}^4 \cdot \text{s}^2$, compared to about $1.55\text{--}1.70 \times 10^{-5} \text{ kg}^2/\text{m}^4 \cdot \text{s}^2$ of the conditioned sludge, which also confirms that agricultural biomass could improve the filterability of sludge and promote the dewatering performance of WAS.

3.3. Sludge rheology changed

The effect of the shear rate on the sludge rheology is shown in Fig. 7. As shown in Fig. 7b, the shear stress obviously increased along with the increase of the shear rate. The Bingham rheology model was applied to analyze the relationship between the shear stress and the shear rate. Some rheological parameters are summarized in Table 5, indicating that the correlation coefficient (R^2) was over 0.96 and revealing the conditioned sludge exhibited similar Pseudoplastic fluids characteristics to the raw sludge (Khongnakorn et al., 2010; Mu and Yu, 2006). As also listed in Table 5, however, the intercept value of the curve (b) of the conditioned sludge was higher than that of the raw sludge, demonstrating that the conditioned sludge behaved poorer in their rheological properties.

As shown in Fig. 7a, moreover, the sludge viscosity sharply declined from about 350–500 mPa·s to almost 60 mPa·s at very low shear rates and then kept almost constant values. The constant viscosity at the infinite shear rate is denoted as the limiting viscosity (u_∞), which represents the viscosity of the sludge matrix corresponding to the maximal dispersion of flocs under the influence of the shear rate (Khongnakorn et al., 2010; Tixier et al., 2003). As listed in Table 5, it is of a great difference in the u_∞ values

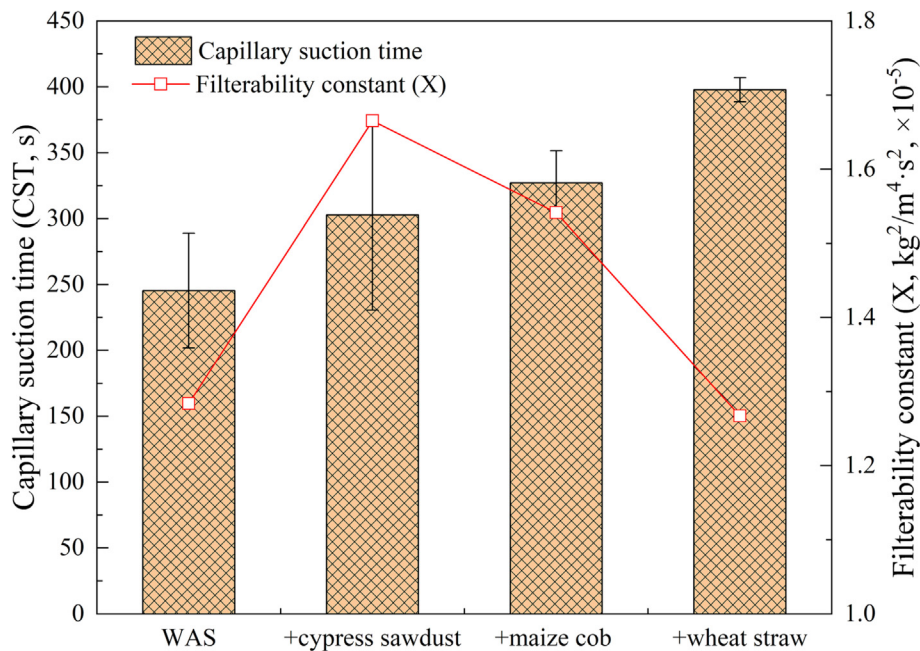
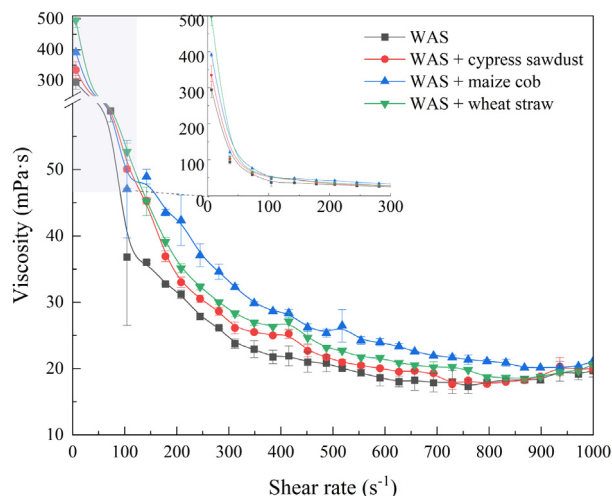
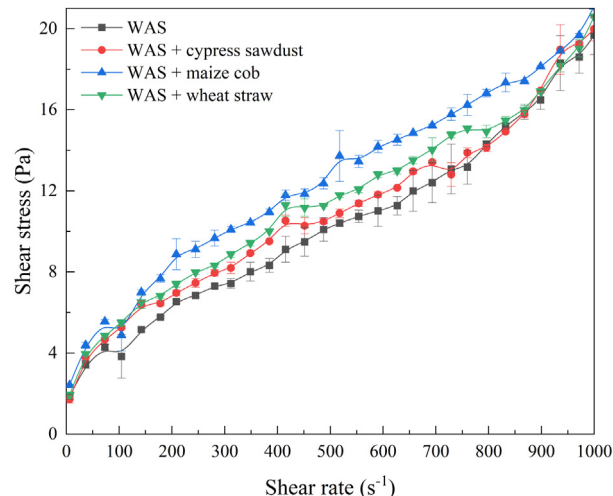


Fig. 6. Capillary suction time (CST) and the filterability constant (X) of the conditioned sludge samples.



(a) Viscosity



(b) Shear stress

Fig. 7. Effect of the shear rate on the rheology of the conditioned sludge samples. a): viscosity; b) shear stress.

of the sludge before and after being conditioned with agricultural biomass ($p < 0.05$). u_{∞} of the raw sludge was about 20.8 ± 1.3 mPa·s, which was lower than the conditioned sludge with cypress sawdust (21.7 ± 0.3 mPa·s), maize cob (25.3 ± 0.6 mPa·s) and wheat straw (23.2 ± 0.2 mPa·s). The conditioned sludge strongly resisted the changed shear rate and was thus forced to form an optimal opening and orientation in the direction of sludge flow (Khongnakorn et al., 2010; Yuan and Wang, 2013). Thus, the interactions inside sludge aggregates would be enhanced, which would benefit to the heat transfer and water release from the inner sludge (Yuan and Wang, 2013).

3.4. Hydrophobicity improved

The hydrophobicity of sludge is associated with different chemical functional groups. FT-IR spectra and different corresponding band assignments are illustrated in Fig. 8 and Table S2. The weaker bands at 2923 cm^{-1} and 2856 cm^{-1} (assigned to C—H vibrations) indicated the lower contents of aliphatic structures and lipids, respectively (Guo et al., 2020). The stronger bands at 1734 cm^{-1} and 1243 cm^{-1} were attributed to more C=O vibration of carboxylic acids and the deformation vibration of C=O in carboxylates, respectively (Cai et al., 2019). These associated groups reflected negative charges on the sludge surface, which would make the conditioned sludge matrix loose and benefit for heat and water transportation. Moreover, the conditioned sludge showed weaker bands at 1645 cm^{-1} and 1544 cm^{-1} , which should be assigned to the deformation of C=O and C—N in the protein amide I group and the stretching vibrations of C—N and N—H in the protein amide II group (Guan et al., 2012; Pei et al., 2020).

The low-abundance of C—N groups were accompanied with the dewaterability improvement due to hydrophilic N-containing functional groups (Xiao et al., 2018). The bands near 1136 cm^{-1} (C—O—C stretching vibrations belonging to carbohydrate) and 1072 cm^{-1} (C—H in-plane bending belonging to polysaccharides) also represented more polysaccharide dominated structures, which means the rich hydrophobic functional

groups in the conditioned sludge samples (Li et al., 2021). All of these results demonstrate that agricultural biomass would strengthen or weaken the associated functional groups, which resulted in higher capacities of water transfer, causing the improvement of the sludge dewaterability and the drying efficiency (Liang and Zhou, 2022).

3.5. Skeleton structures reshaped

The surface structures of the sludge samples were recorded by SEM images, as depicted in Fig. 9. The conditioned sludge obviously presented the complicated pores and/or skeleton structures, which were very different from the matrix structures of the raw sludge. The conditioned sludge with cypress sawdust (Fig. 9b) had a sponge-like structure with many large cracks and pores. The conditioned sludge with maize cobs (Fig. 9c) formed a lumpy structure that enhanced small particles to adhere to cobs, thus forming a water transfer channel with the rigid skeleton structure on the surface of flocs. As shown in Fig. 9d, on the other hand, wheat straw in the conditioned sludge directly played a role of the skeleton and thus formed a mesh-like structure, which increased the hardness and thus decreased the sludge compressibility. Moreover, the rough and irregular prongs of wheat straw pelt off the extracellular polymeric substances and even punctured the wall of bacterial cells (Liu et al., 2017). Above all, the sludge porosity was improved by agricultural biomass and special channels were formed, which could facilitate the heat and water transfer channels within the sludge.

Anyway, different agricultural biomass played different roles in reforming sludge structures, which were responsible for different promoted efficiency and mechanisms on the drying performance. The order of different agricultural biomass on forming sludge skeleton was: wheat straw > cypress sawdust > maize cob. Maize cobs mainly formed the network structure, and cypress sawdust would increase the crevices in sludge flocs, while wheat straw could improve the roughness of sludge in both radial and lateral directions for promoting water transfers. That is why wheat straw could achieve the best enhancement performance on drying sludge than others.

3.6. Particle size enlarged

As shown in Fig. 10, the particle size distribution of the conditioned sludge indicates that agricultural biomass obviously affected the particle size of the sludge. The mean diameter of the volume (MV) increased from $46.3\text{ }\mu\text{m}$ (the raw sludge) to around $120\text{ }\mu\text{m}$ (the conditioned sludge with cypress sawdust and maize cobs), and even to $214.4\text{ }\mu\text{m}$ for the conditioned

Table 5
Rheological parameters of the conditioned sludge samples.

Samples	Limiting viscosity (u_{∞} , mPa·s)	Shear stress		
		k	b	R ²
Raw WAS	20.8 ± 1.3	0.0155	2.5447	0.980
WAS + cypress sawdust	21.7 ± 0.3	0.0151	3.3487	0.969
WAS + maize cob	25.3 ± 0.6	0.0159	4.5047	0.980
WAS + wheat straw	23.2 ± 0.2	0.0152	3.8037	0.979

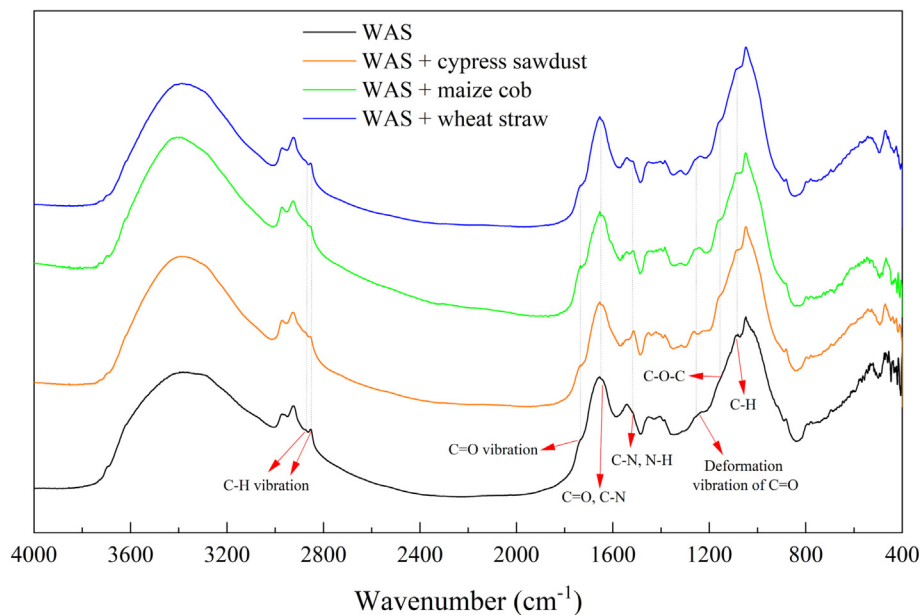


Fig. 8. Fourier transform infrared (FT-IR) spectra of the conditioned sludge samples.

sludge with wheat straw. Higgins and Novak (1997) stated that the particles over 100 μm had a positive influence on the dewaterability of sludge. Particle diameter representing cumulative 50 % distribution ($D[50]$) also increased from 37.3 μm to 45.0 μm (with cypress sawdust and maize cob) and 58.3 μm (wheat straw), which means that added agricultural biomass could enlarge sludge particle size and form more dispersed structures and

thus could enhance the dewaterability of sludge. This conclusion was also supported by the skeleton structures, as shown in SEM images (Fig. 9).

Moreover, the strength factor (S_f) (the ratio of the MV value of the conditioned sludge to the raw sludge) was also calculated and listed in Fig. 10. The S_f values were all over 1.0, which indicates that the conditioned sludge was better to withstand shear rate and thus formed more network

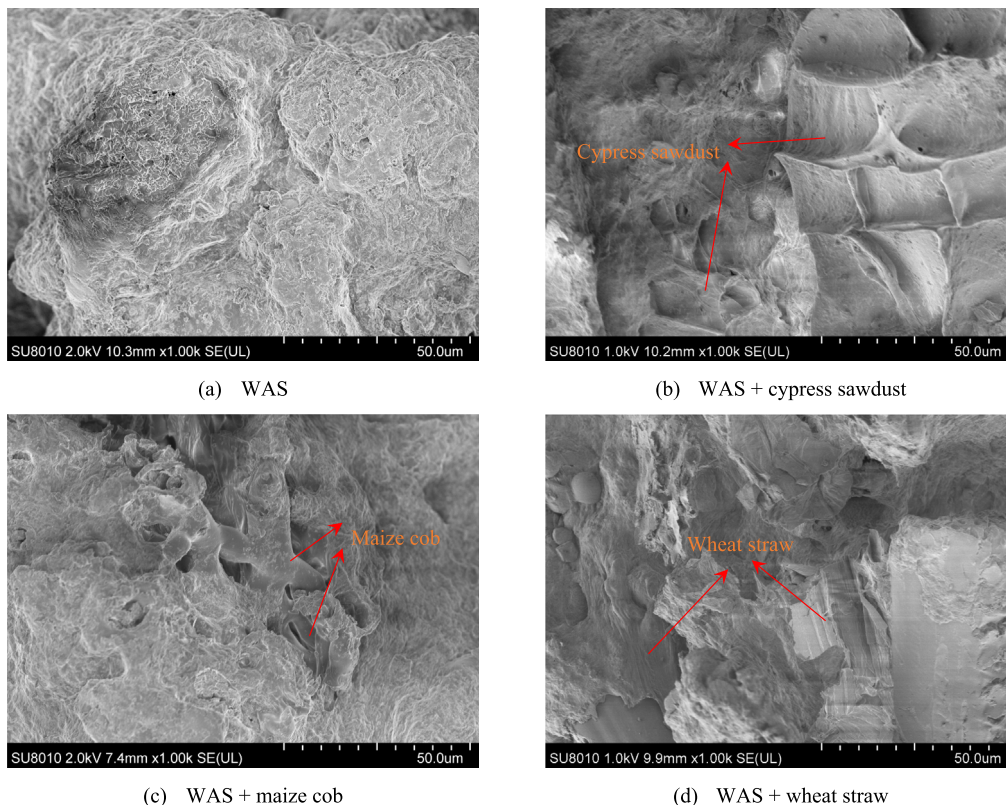


Fig. 9. Microscopic morphology using scanning electron microscope (SEM) (magnification $\times 1.0$ k): a) WAS; b) WAS + cypress sawdust; c) WAS + maize cob; d) WAS + wheat straw.

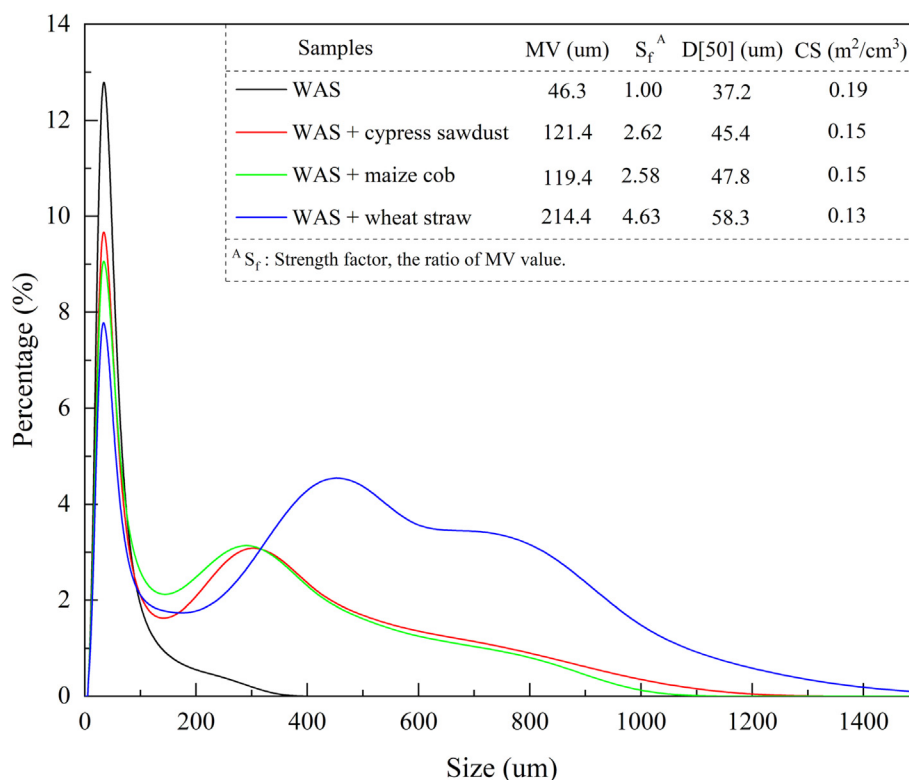


Fig. 10. Particle size distribution of the sludge samples conditioned with agricultural biomass.

structures. These results were consistent with the analysis of sludge rheology (Cao et al., 2016). Among them, the highest S_f value (4.63) for the conditioned sludge with wheat straw demonstrated the best effective influence on the sludge drying performance.

The calculated specific surface area (CS) in Fig. 10 showed a slight decrease from $0.19 m^2/cm^3$ (the raw sludge) to $0.13 m^2/cm^3$ (the conditioned sludge). These fluffy structures were more conducive to the water release and heat transfer during the drying process. It was noteworthy that particle size distribution and skeletal structure formation between cypress sawdust and maize cob were essentially similar, which explained the phenomena of the same enhancement on the sludge drying performance.

4. Conclusions

To enhance the drying performance, waste activated sludge (WAS) was conditioned by the agricultural biomass: cypress sawdust, maize cob and wheat straw. The drying performance and associated mechanisms were fully analyzed and some conclusions can be drawn below:

- Three kinds of agricultural biomass could all improve the performance of low-temperature sludge drying. Among them, wheat straw achieved the highest enhanced efficiency.
- 20 % of crushed wheat straw (DS/DS) was proposed as an appropriate ratio, which was associated with the average drying rate of 0.20 g water/g DS·min, higher than that of the raw sludge (0.13 g water/g DS·min). Moreover, the drying time reaching the targeted moisture content for self-supporting incineration was only 12.0 min, about half of the raw sludge (21 min).
- The sludge dewaterability was enhanced as SRF decreased (from $6.38 \times 10^{12} m/kg$ to around $1.80 \times 10^{12} m/kg$) and filterability (X) increased (from $1.28 \times 10^{-5} kg^2/m^4 \cdot s^2$ to $1.67 \times 10^{-5} kg^2/m^4 \cdot s^2$).
- The conditioned sludge was poor in the rheology properties along with increasing shear stress and viscosity.
- Biomass played a role of the skeleton to form a large amount of lumpy and/or mesh-like structures with sludge matrix, which could provide preferable channels to transfer the heat and water.

CRediT authorship contribution statement

Ji Li: Conceptualization, Methodology, Formal analysis, Investigation, Writing - Original draft preparation. Xiaodi Hao: Supervision, Writing - Reviewing and Editing, Project administration. Zhan Shen: Investigation, Writing - Original draft preparation. Yuanyuan Wu: Resources. Mark C. M. van Loosdrecht: Supervision.

Data availability

Data will be made available on request.

Declaration of competing interest

The authors declare that they have no known competing financial interests or personal relationships that could have appeared to influence the work reported in this paper.

Acknowledgement

The study was financially supported by the National Natural Science Foundation of China (52170018), and Beijing Energy Conservation & Sustainable Urban and Rural Development Provincial and Ministry Co-construction Collaboration Innovation Center (2023).

Appendix A. Supplementary data

Supplementary data to this article can be found online at <https://doi.org/10.1016/j.scitotenv.2023.164200>.

References

- Agerbaek, M.L., Keiding, K., 1993. On the origin of specific resistance to filtration. Water Sci. Technol. 28, 159–168. <https://doi.org/10.2166/wst.1993.0039>.
- APHA, 2012. Standard Methods for the Examination of Water and Wastewater. 20th Ed. American Public Health Association, Washington, D.C.

- Cai, M., Wang, Q., Wells, G., Dionysiou, D.D., Song, Z., Jin, M., Hu, J., Ho, S.H., Xiao, R., Wei, Z., 2019. Improving dewaterability and filterability of waste activated sludge by electrochemical Fenton pretreatment. *Chem. Eng. J.* 362, 525–536. <https://doi.org/10.1016/j.cej.2019.01.047>.
- Cao, B., Zhang, W., Wang, Q., Huang, Y., Meng, C., Wang, D., 2016. Wastewater sludge dewaterability enhancement using hydroxyl aluminum conditioning: role of aluminum speciation. *Water Res.* 105, 615–624. <https://doi.org/10.1016/j.watres.2016.09.016>.
- Cao, B., Zhang, T., Zhang, W., Wang, D., 2021. Enhanced technology based for sewage sludge deep dewatering: a critical review. *Water Res.* 189, 116650. <https://doi.org/10.1016/j.watres.2020.116650>.
- Cetin, S., Erdinciler, A., 2004. The role of carbohydrate and protein parts of extracellular polymeric substances on the dewaterability of biological sludges. *Water Sci. Technol.* 50, 49–56.
- Chen, Z., Zhang, W., Wang, D., Ma, T., Bai, R., 2015. Enhancement of activated sludge dewatering performance by combined composite enzymatic lysis and chemical reflocculation with inorganic coagulants: kinetics of enzymatic reaction and reflocculation morphology. *Water Res.* 83, 367–376. <https://doi.org/10.1016/j.watres.2015.06.026>.
- Donatello, S., Cheeseman, C.R., 2013. Recycling and recovery routes for incinerated sewage sludge ash (ISSA): a review. *Waste Manag.* 33, 2328–2340. <https://doi.org/10.1016/j.wasman.2013.05.024>.
- Guan, B., Yu, J., Fu, H., Guo, M., Xu, X., 2012. Improvement of activated sludge dewaterability by mild thermal treatment in CaCl₂ solution. *Water Res.* 46, 425–432. <https://doi.org/10.1016/j.watres.2011.11.014>.
- Guo, J., Jia, X., Gao, Q., 2020. Insight into the improvement of dewatering performance of waste activated sludge and the corresponding mechanism by biochar-activated persulfate oxidation. *Sci. Total Environ.* 744, 140912. <https://doi.org/10.1016/j.scitotenv.2020.140912>.
- Hao, X., Chen, Q., Van Loosdrecht, M.C.M., Li, J., Jiang, H., 2020. Sustainable disposal of excess sludge : incineration without anaerobic digestion. *Water Res.* 170. <https://doi.org/10.1016/j.watres.2019.115298>.
- Hao, X., Li, J., van Loosdrecht, M.C.M., Jiang, H., Liu, R., 2019. Energy recovery from wastewater: heat over organics. *Water Res.* 161, 74–77. <https://doi.org/10.1016/j.watres.2019.05.106>.
- Hao, X., Wang, X., Shi, C., van Loosdrecht, M.C.M., Wu, Y., 2022. Creating coagulants through the combined use of ash and brine. *Sci. Total Environ.* 845, 157344. <https://doi.org/10.1016/j.scitotenv.2022.157344>.
- Higgins, M.J., Novak, J.T., 1997. The effect of cations on the settling and dewatering of activated sludges: laboratory results. *Water Environ. Res.* 69, 215–224. <https://doi.org/10.2175/106143097x125371>.
- Khongnakorn, W., Mori, M., Vachoud, L., Delalande, M., Wisniewski, C., 2010. Rheological properties of SBR sludge under unsteady state conditions. *Desalination* 250, 824–828. <https://doi.org/10.1016/j.desal.2008.11.050>.
- Komilis, D., Kissas, K., Symeonidis, A., 2014. Effect of organic matter and moisture on the calorific value of solid wastes: an update of the Tanner diagram. *Waste Manag.* 34, 249–255. <https://doi.org/10.1016/j.wasman.2013.09.023>.
- Li, J., Hao, X., Gan, W., van Loosdrecht, M.C.M., Wu, Y., 2021. Recovery of extracellular biopolymers from conventional activated sludge: potential, characteristics and limitation. *Water Res.* 205, 117706. <https://doi.org/10.1016/j.watres.2021.117706>.
- Li, W.W., Sheng, G.P., Zeng, R.J., Liu, X.W., Yu, H.Q., 2012. China's wastewater discharge standards in urbanization: evolution, challenges and implications: evolution, challenges and implications. *Environ. Sci. Pollut. Res.* 19, 1422–1431. <https://doi.org/10.1007/s11356-011-0572-7>.
- Liang, J., Zhou, Y., 2022. Iron-based advanced oxidation processes for enhancing sludge dewaterability : state of the art, challenges, and sludge reuse. *Water Res.* 218, 118499. <https://doi.org/10.1016/j.watres.2022.118499>.
- Lin, Y.F., Jing, S.R., Lee, D.Y., 2001. Recycling of wood chips and wheat dregs for sludge processing. *Bioresour. Technol.* 76, 161–163. [https://doi.org/10.1016/S0960-8524\(00\)00098-5](https://doi.org/10.1016/S0960-8524(00)00098-5).
- Liu, Hongbo, Xiao, H., Fu, B., Liu, He, 2017. Feasibility of sludge deep-dewatering with sawdust conditioning for incineration disposal without energy input. *Chem. Eng. J.* 313, 655–662. <https://doi.org/10.1016/j.cej.2016.09.107>.
- Liu, H., Yang, J., Zhu, N., Zhang, H., Li, Y., He, S., Yang, C., Yao, H., 2013. A comprehensive insight into the combined effects of Fenton's reagent and skeleton builders on sludge deep dewatering performance. *J. Hazard. Mater.* 258–259, 144–150. <https://doi.org/10.1016/j.jhazmat.2013.04.036>.
- Mu, Y., Yu, H.-Q., 2006. Rheological and fractal characteristics of granular sludge in an upflow anaerobic reactor. *Water Res.* 40, 3596–3602. <https://doi.org/10.1016/j.watres.2006.05.041>.
- Niu, M., Zhang, W., Wang, D., Chen, Y., Chen, R., 2013. Correlation of physicochemical properties and sludge dewaterability under chemical conditioning using inorganic coagulants. *Bioresour. Technol.* 144, 337–343. <https://doi.org/10.1016/j.biortech.2013.06.126>.
- Olga, M., Laila, D., Oleg, K., Jana, C., Ina, A., 2022. Application of the sewage sludge in agriculture: soil fertility, technoeconomic, and life-cycle assessment. *Hazard. Waste Manag.* 1–26 Chapter.
- Pei, K., Xiao, K., Hou, H., Tao, S., Xu, Q., Liu, B., Yu, Z., Yu, W., Wang, H., Xue, Y., Liang, S., Hu, J., Deng, H., Yang, J., 2020. Improvement of sludge dewaterability by ammonium sulfate and the potential reuse of sludge as nitrogen fertilizer. *Environ. Res.* 191. <https://doi.org/10.1016/j.envres.2020.110050>.
- Qi, Y., Thapa, K.B., Hoadley, A.F.A., 2011. Application of filtration aids for improving sludge dewatering properties - a review. *Chem. Eng. J.* 171, 373–384. <https://doi.org/10.1016/j.cej.2011.04.060>.
- Tahmasebi, A., Yu, J., Li, X., Meesri, C., 2011. Experimental study on microwave drying of Chinese and Indonesian low-rank coals. *Fuel Process. Technol.* 92, 1821–1829. <https://doi.org/10.1016/j.fuproc.2011.04.004>.
- Tixier, N., Guibaud, G., Baudu, M., 2003. Determination of some rheological parameters for the characterization of activated sludge. *Bioresour. Technol.* 90, 215–220. [https://doi.org/10.1016/S0960-8524\(03\)00109-3](https://doi.org/10.1016/S0960-8524(03)00109-3).
- Vesilind, P.A., 1988. Capillary suction time as a fundamental measure of sludge dewaterability. *J. Water Pollut. Control Fed.* 60, 215–220.
- Wang, X., Shi, C., Hao, X., van Loosdrecht, M.C.M., Wu, Y., 2023. Synergy of phosphate recovery from sludge-incinerated ash and coagulant production by desalinated brine. *Water Res.* 231, 119658. <https://doi.org/10.1016/j.watres.2023.119658>.
- Wang, T., Shi, F., Zhang, Q., Qian, X., Hashimoto, S., 2018. Exploring material stock efficiency of municipal water and sewage infrastructures in China. *J. Clean. Prod.* 181, 498–507. <https://doi.org/10.1016/j.jclepro.2018.01.253>.
- Wu, B., Dai, X., Chai, X., 2020. Critical review on dewatering of sewage sludge: influential mechanism, conditioning technologies and implications to sludge re-utilizations. *Water Res.* 180, 115912. <https://doi.org/10.1016/j.watres.2020.115912>.
- Wu, Y., Zhang, P., Zhang, H., Zeng, G., Liu, J., Ye, J., Fang, W., Gou, X., 2016. Possibility of sludge conditioning and dewatering with rice husk biochar modified by ferric chloride. *Bioresour. Technol.* 205, 258–263. <https://doi.org/10.1016/j.biortech.2016.01.020>.
- Xiao, K., Pei, K., Wang, H., Yu, W., Liang, S., Hu, J., Hou, H., Liu, B., Yang, J., 2018. Citric acid assisted Fenton-like process for enhanced dewaterability of waste activated sludge with in-situ generation of hydrogen peroxide. *Water Res.* 140, 232–242. <https://doi.org/10.1016/j.watres.2018.04.051>.
- Xiao, Z., Yuan, X., Jiang, L., Chen, X., Li, H., Zeng, G., Leng, L., Wang, H., Huang, H., 2015. Energy recovery and secondary pollutant emission from the combustion of co-pelletized fuel from municipal sewage sludge and wood sawdust. *Energy* 91, 441–450. <https://doi.org/10.1016/j.energy.2015.08.077>.
- Yang, Q., Yi, J., Luo, K., Jing, X., Li, X., Liu, Y., Zeng, G., 2013. Improving disintegration and acidification of waste activated sludge by combined alkaline and microwave pretreatment. *Process. Saf. Environ. Prot.* 91, 521–526. <https://doi.org/10.1016/j.psep.2012.12.003>.
- Yuan, D., Wang, Y., 2013. Influence of extracellular polymeric substances on rheological properties of activated sludge. *Biochem. Eng. J.* 77, 208–213. <https://doi.org/10.1016/j.bej.2013.06.011>.
- Zhang, W., Xiao, P., Liu, Y., Xu, S., Xiao, F., Wang, D., Chow, C.W.K., 2014. Understanding the impact of chemical conditioning with inorganic polymer flocculants on soluble extracellular polymeric substances in relation to the sludge dewaterability. *Sep. Purif. Technol.* 132, 430–437. <https://doi.org/10.1016/j.seppur.2014.05.034>.
- Zhang, Q.H., Yang, W.N., Ngo, H.H., Guo, W.S., Jin, P.K., Dzakupasu, M., Yang, S.J., Wang, Q., Wang, X.C., Ao, D., 2016. Current status of urban wastewater treatment plants in China. *Environ. Int.* 92–93, 11–22. <https://doi.org/10.1016/j.envint.2016.03.024>.